Charge separation and (triplet) recombination in diketopyrrolopyrrole-fullerene triads

Karsten, Bram P.; Bouwer, Ricardo K. M.; Hummelen, Jan C.; Williams, Rene M.; Janssen, Rene A. J.

Published in:
Photochemical & Photobiological Sciences

DOI:
10.1039/c0pp00098a

Publication date:
2010

Charge separation and (triplet) recombination in diketopyrrolopyrrole–fullerene triads†

Bram P. Karsten,[a] Ricardo K. M. Bouwer,[b,c] Jan C. Hummelen,[b] René M. Williams[d] and René A. J. Janssen*[a,c]

Received 20th April 2010, Accepted 18th May 2010
First published as an Advance Article on the web 7th June 2010
DOI: 10.1039/c0pp00098a

Synthesis and photophysics of two diketopyrrolopyrrole-based small band gap oligomers, end-capped at both ends with C_{60} are presented. Upon photoexcitation of the oligomer, ultrafast energy transfer to the fullerene occurs (~0.5 ps), followed by an electron transfer reaction. Femtosecond transient absorption has been used to determine the rates for charge separation and recombination. Charge separation occurs in the Marcus normal region with a time constant of 18–47 ps and recombination occurs in the inverted regime, with a time constant of 37 ps to 1.5 ns. Both processes are faster in *o*-dichlorobenzene (ODCB) than in toluene. Analysis of the charge transfer rates by Marcus-Jortner theory leads to the view that the positive charge must be located on the thiophene/dithiophene unit closest to the fullerene. Approximately 14% of the charge transfer state was found to recombine into the low-lying triplet state of the oligomer for the smaller system in ODCB.

Introduction

Photovoltaics are considered as one of the viable options for future energy supplies. In this respect, organic photovoltaics are regarded as an attractive alternative for the inorganic solar cells used at present, due to their flexibility, ease of processing and potentially low cost. In recent years, many different polymers have been reported as active materials and the best efficiencies to date approach 7.5%, when combined with fullerene derivatives in bulk heterojunction devices.[1–4]

One class of compounds that has attracted much interest recently is based on alternating electron-rich thiophene units and electron-poor diketopyrrolopyrrole (DPP) units. This alternation of electron-rich and electron-poor units in the main chain generally reduces the band gap of conjugated polymers, giving rise to strong light absorption extending into the near-infrared region of the spectrum. Using polymers[5–8] and short oligomers[9–11] containing the DPP unit, device efficiencies approaching 5% have been reported. A common feature of these DPP-based materials is their relatively high oxidation potential, leading to high-energy charge separated states when combined with fullerenes, and to correspondingly high voltages when used in solar cells.

Despite the advantage of having light absorption extending into the near-IR region of the spectrum, one of the drawbacks of small-band gap systems like the DPP-based polymers is their generally low triplet energy. If the triplet energy is lower than the energy of the charge separated state, this leads to the possibility of charge recombination into the triplet state. This triplet recombination is therefore likely to be a loss mechanism in solar cells based on small band gap polymers and oligomers.[12–14]

As electron transfer reactions are key steps in the charge separation and recombination processes, detailed knowledge about these reactions could be of great help in designing new donor–acceptor combinations. Many studies of electron transfer processes in linked donor-fullerene systems have been performed in past decades.[15–43] In general, charge separation occurs rapidly, in the Marcus-normal regime, followed by charge recombination in the Marcus inverted regime. Also charge recombination into a triplet state has been observed frequently.[15,18,44–47]

We recently reported studies on several small band gap oligomer–fullerene triads, using thienopyrazines (TPs) as the electron-deficient unit in the oligomer.[48] Consistent with previous studies,[15–43] very fast charge separation in the C_{60}-TP-C_{60} triads took place close to the Marcus optimal region, while charge recombination occurred in the Marcus inverted region. In the C_{60}-TP-C_{60} triads no recombination into the low-lying triplet state could be observed, most probably due to the short lifetime of the charge separated state, preventing intersystem crossing in that state. Here, we present a similar series of oligomer–fullerene triads, based on the DPP-core as the electron-deficient unit in the oligomers. In these systems, charge transfer takes place in a two-step fashion, upon photoexitation of the oligomer. In the first step, energy transfer to the C_{60} moiety takes place, followed by electron transfer in the Marcus normal region. As the energy of the charge separated state in the DPP-systems is higher than in the TP-systems, and charge recombination takes place in the Marcus inverted regime, the lifetime of the charge separated state is long enough to allow relatively slow intersystem crossing followed by

[a]*Molecular Materials and Nanosystems, Eindhoven University of Technology, P.O. Box 513, 5600 MB, Eindhoven, The Netherlands. E-mail: r.a.j.janssen@tue.nl.*
[b]*Molecular Electronics, Stratingh Institute for Chemistry and Zernike Institute for Advanced Materials, University of Groningen, Nijenborgh 4, 9747 AG, Groningen, The Netherlands*
[c]*Dutch Polymer Institute (DPI), P.O. Box 902, 5600 AX, Eindhoven, The Netherlands*
[d]*Molecular Photonics Group, Van't Hoff Institute for Molecular Sciences, Universiteit van Amsterdam, Nieuwe Achtergracht 129, 1018 WS, Amsterdam, The Netherlands*

† This article is published as part of a themed issue in appreciation of the many important contributions made to the field of molecular photophysics by Jan Verhoeven.

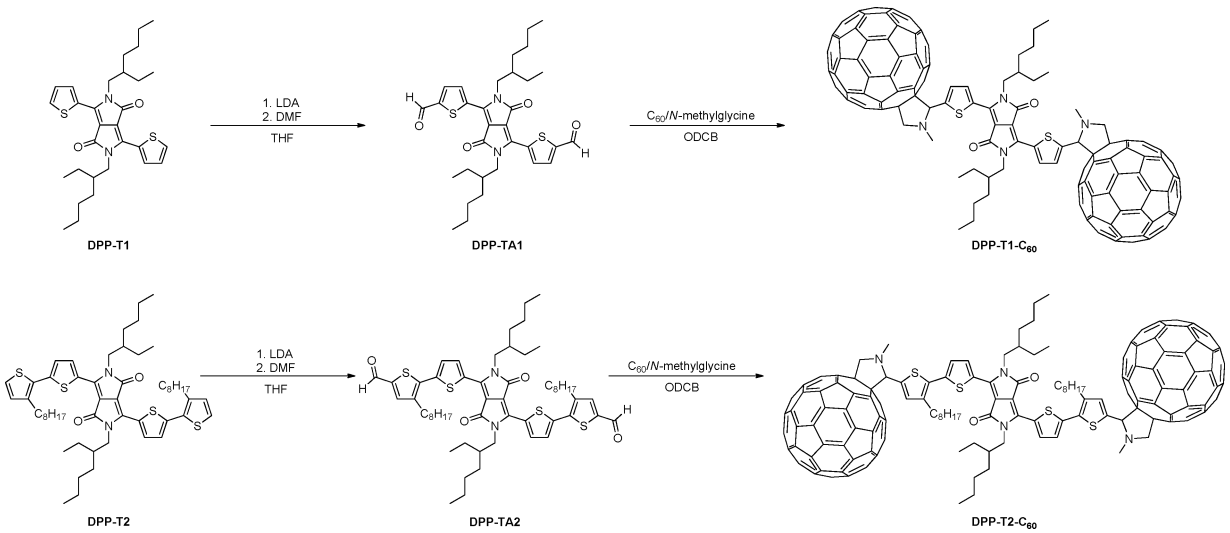

Scheme 1 Synthesis of the compounds under study.

much faster charge recombination into the triplet excited state of the oligomer.

Results and discussion

Synthesis

Synthesis of the compounds is depicted in Scheme 1. Oligomers **DPP-T1** and **DPP-T2** were synthesized according to (modified) literature procedures.[7,49] Lithiation with lithium diisopropylamide (LDA), followed by quenching of the anion by *N*,*N*-dimethylformamide (DMF) gave the corresponding aldehydes. These were reacted with C_{60} and *N*-methylglycine in a Prato reaction,[50] yielding triads **DPP-T1-C_{60}** and **DPP-T2-C_{60}**. Small amounts of the crude triads were purified by preparative HPLC for the analysis described in this work. The compounds were characterized by ^{1}H-NMR, ^{13}C-NMR, FT-IR and MALDI-TOF-MS.

Optical and electrochemical properties

UV/vis absorption spectra of the oligomers and triads are given in Fig. 1a. It can be seen, that the absorption of the triads resembles a superposition of the spectra of the separate oligomer and *N*-methylfulleropyrrolidine (MP-C_{60}) units, although a distinct red-shift in the absorption is observed. The most likely cause for this red-shift is the fact that the end-groups connected to the oligomer (H in the bare oligomer and MP-C_{60} in the triads) differ, thereby slightly influencing the electronic energy levels of the polymer. No other electronic interactions (*e.g.* charge-transfer absorptions) can be observed in the absorption spectrum of **DPP-T2-C_{60}**. Due to the low solubility of **DPP-T1-C_{60}**, some scattering occurred in the UV-experiment, reflected in the low-energy tail of the spectrum. Therefore, no definite conclusions about other electronic interactions can be drawn from these spectra, although there are no clear indications for their existence. From the onsets of absorption, the optical band gaps of the oligomers can be calculated as 2.15 eV for **DPP-T1** and 1.88 eV for **DPP-T2**. The UV/vis absorption data of the oligomers are summarized in Table 1.

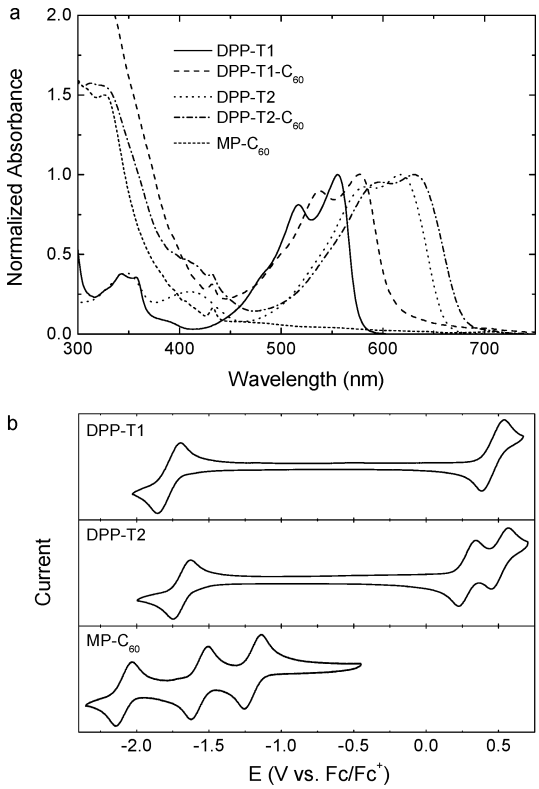

Fig. 1 Normalized UV/vis absorption spectra of the oligomers, triads and MP-C_{60} recorded in ODCB (a) and cyclic voltammograms of the oligomers and MP-C_{60} recorded in ODCB (b).

Cyclic voltammograms of the separate oligomers and MP-C_{60} are depicted in Fig. 1b. In both oligomers, one or two reversible oxidations and one reversible reduction were observed. From the onsets of oxidation and reduction, the electrochemical band gaps of the oligomers can be calculated as 2.09 eV for **DPP-T1**, and 1.81 eV for **DPP-T2**. These values are in good agreement with the optical band gaps. The electrochemical data for the oligomers are summarized in Table 1.

Table 1 UV/vis absorption and fluorescence and electrochemical data in ODCB for the oligomers and MP-C_{60}. Oxidation and reduction potentials are relative to ferrocene

	λ_{onset}/nm	E_{S1}/eV	λ_{max}/nm	λ_{max}^{PL}/nm	Φ_F	τ_F/ns	E_{ox}^{onset}/V	$E_{ox}°$/V	E_{red}^{onset}/V	$E_{red}°$/V	E_g^{CV}/eV
DPP-T1	576	2.15	555	569	0.62	5.9	0.38	0.46	–1.71	–1.78	2.09
DPP-T2	660	1.88	617	653	>0.23[a]	2.5	0.21	0.29	–1.60	–1.69	1.81
MP-C_{60}	726	1.71	433	717		1.3			–1.13	–1.20	

[a] The full fluorescence band could not be detected. Therefore, a lower limit for the fluorescence quantum yield is given.

Triplet excited states and cations of the oligomers

The absorptions of the triplet excited states of **DPP-T1** and **DPP-T2** were investigated by near steady-state photoinduced absorption (PIA) spectroscopy. As direct excitation of the oligomers did not result in a detectable signal, due to the low quantum yield for intersystem crossing to the triplet state, triplet sensitization with MP-C_{60} in toluene solution was employed.[51] In these experiments MP-C_{60} was excited, leading to the triplet excited state of MP-C_{60} with a quantum yield of near unity. The energy of this triplet state can then be transferred from MP-C_{60} to the oligomer, provided that the latter triplet state has a lower energy than the triplet of MP-C_{60}. The obtained spectra are shown in Fig. 2. Both spectra show a bleaching band at the absorption wavelength of the oligomer, and a strong absorption at lower energy. The triplet spectrum of **DDP-T1** shows a $T_n \leftarrow T_1$ absorption at 1.44 eV with two vibronic progressions to higher energies with spacings of 0.16 (strong) and 0.08 eV (weak). In **DPP-T2** the lowest energy $T_n \leftarrow T_1$ absorption has red shifted to 1.08 eV, again with a vibronic peak shifted by 0.16 eV, but the spectrum is dominated by an absorption at 1.88 eV.

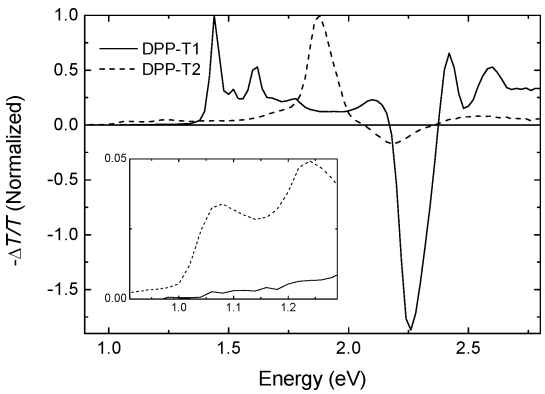

Fig. 2 Near steady-state PIA spectra of mixtures of **DPP-T1** or **DPP-T2** (0.1 mM) and MP-C_{60} (0.4 mM) recorded in toluene, at an excitation wavelength of 351/364 nm. The inset shows an enlargement of the low-energy part of the spectra.

The energies of the triplet states can be estimated by adding quenchers with a known triplet energy to the oliogomer/MP-C_{60} mixture. If the triplet energy of the oligomer is lower than the triplet energy of the quencher, the spectrum is not affected and the triplet state of the oligomer is still visible. If however, the triplet energy of the quencher is lower than that of the oligomer, the triplet of the oligomer is quenched, and the triplet absorption of the quencher is observed. In case both absorptions are visible, both triplets have about the same energy. In this way, the energies of the triplet states of the oligomers can be estimated as being around 1.1 eV for **DPP-T1** (partial quenching of the rubrene triplet, at 1.14 eV,[52] and visibility of both **DPP-T1** and rubrene triplet signals in the spectrum) and around 0.9 eV for **DPP-T2** (partial quenching of the bis(trihexylsiloxy)silicon-2,3-naphthalocyanine triplet, at 0.93 eV).[53] The triplet energy of MP-C_{60} is known to be 1.50 eV.[15] Triplet energies and absorption maxima are summarized in Table 2.

Table 2 Triplet $T_n \leftarrow T_1$ absorption maxima and triplet energies (E_T) of the oligomers and absorption maxima ($D_1 \leftarrow D_0$ and $D_2 \leftarrow D_0$) of the oxidized oligomers

	$T_n \leftarrow T_1$/eV	E_T/eV	RC $D_1 \leftarrow D_0$/eV	RC $D_2 \leftarrow D_0$/eV
DPP-T1	1.44	1.1	1.45	2.03
DPP-T2	1.08 1.88	0.9	1.21	1.45

The absorption spectra of the radical cations, formed upon oxidation of **DPP-T1** and **DPP-T2** can be investigated by chemical oxidation with thianthrenium hexafluorophosphate.[54] In these experiments the oxidant is added to a solution of the oligomer in small aliquots, and the UV/vis spectra are recorded. Spectra obtained in this way are shown in Fig. 3. In both cases, the original

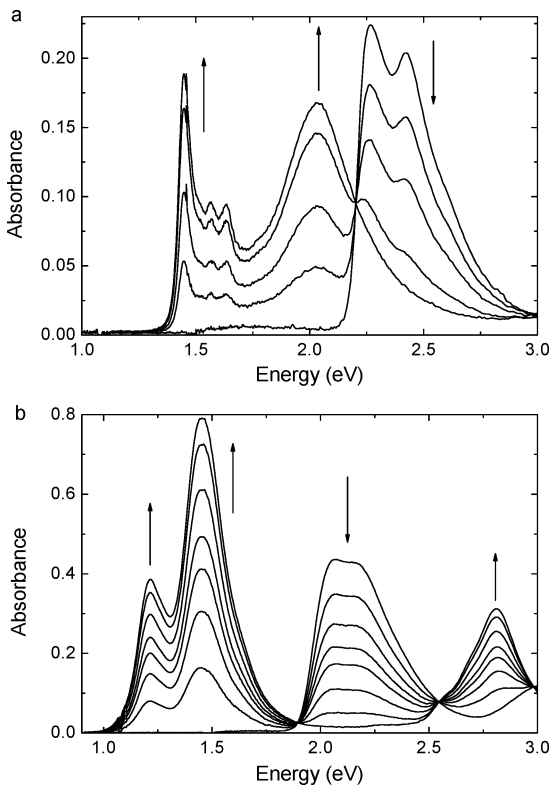

Fig. 3 Chemical oxidation of oligomers **DPP-T1** (a) and **DPP-T2** (b) by adding a solution of thianthrenium hexafluorophosphate. The appearance and disappearance of bands is indicated with arrows.

$\pi \rightarrow \pi^*$ absorption band of the neutral oligomer disappears and two bands appear at lower energy. These bands can be attributed to the HOMO→SOMO (Singly Occupied Molecular Orbital) and SOMO→LUMO transitions of the newly formed doublet-state radical. The absorption maxima of the radical cations are summarized in Table 2.

Photoluminescence of oligomers and triads

Photoluminescence spectra of oligomers **DPP-T1** and **DPP-T2** dissolved in toluene are depicted in Fig. 4a. Fluorescence maxima, quantum yields and lifetimes are summarized in Table 1. Whereas the bare oligomers are strongly fluorescent, the fluorescence of the DPP oligomer in the triads is fully quenched due to the very fast decay of the S_1 state of the DPP moiety, either by energy transfer to the C_{60} units or by electron transfer from the C_{60} to the DPP oligomer.

Some insight into the processes occurring after excitation can be obtained, when the fluorescence of the C_{60} units is examined. Quenching of the fluorescence of MP-C_{60} in the triads is shown in Fig. 4b. For this graph, MP-C_{60} and the oligomers were excited at 433 nm, corresponding to the small absorption maximum in the fullerene spectrum, and the emission spectra of all compounds were recorded without changing the settings of the spectrometer. The spectra were corrected for the optical density at the excitation wavelength, and hence the height of the fluorescent peaks is proportional to the relative quantum yields for fluorescence of the different compounds. It is clear from Fig. 4b that in toluene, the fluorescence of the C_{60}-units is partially quenched (~55% for **DPP-T1-C_{60}** and ~75% for **DPP-T2-C_{60}**), indicating some, but incomplete, charge transfer in these systems. In ODCB quenching of the C_{60} fluorescence is nearly complete for **DPP-T1-C_{60}** and **DPP-T2-C_{60}**, indicating efficient charge separation as a result of the higher solvent polarity that stabilizes the charge separated state.

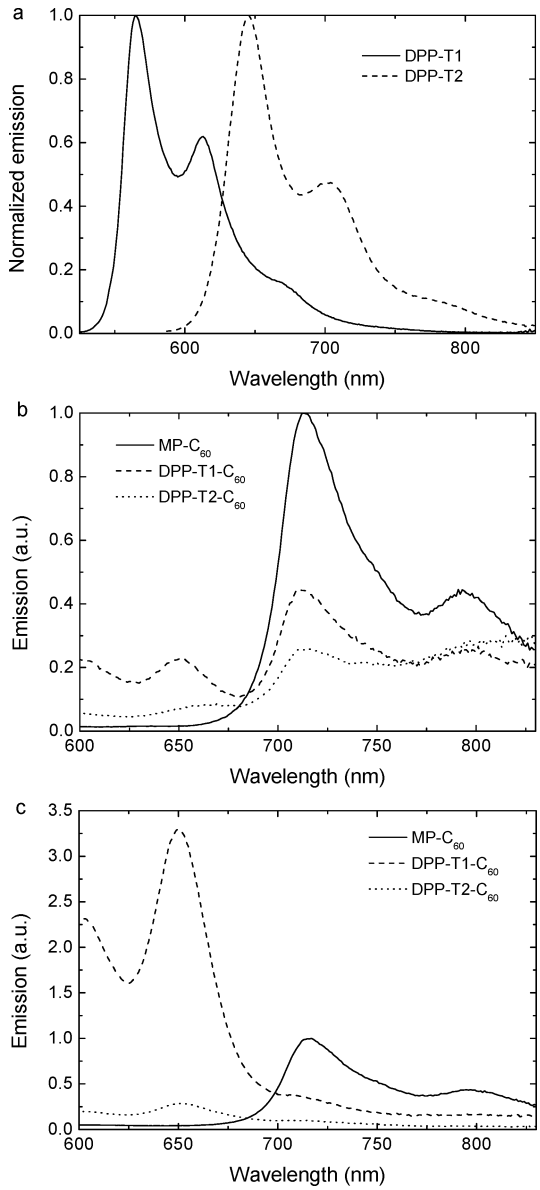

Fig. 4 Normalized photoluminescence spectra of the oligomers in toluene (a) and quenching of the fullerene fluorescence in the triads in toluene (b) and ODCB (c), recorded with excitation at 433 nm.

Charge separation and recombination processes

Near steady-state PIA spectra of the triads **DPP-T1-C_{60}** and **DPP-T2-C_{60}** are shown in Fig. 5. For both oligomers, clear signals are observed in both toluene and ODCB that can be attributed to the absorption of the triplet excited state of the DPP-oligomers. As the bare oligomers do not show any detectable amount of triplet absorptions, the observed triplet states must be formed *via* another process than direct intersystem crossing from the

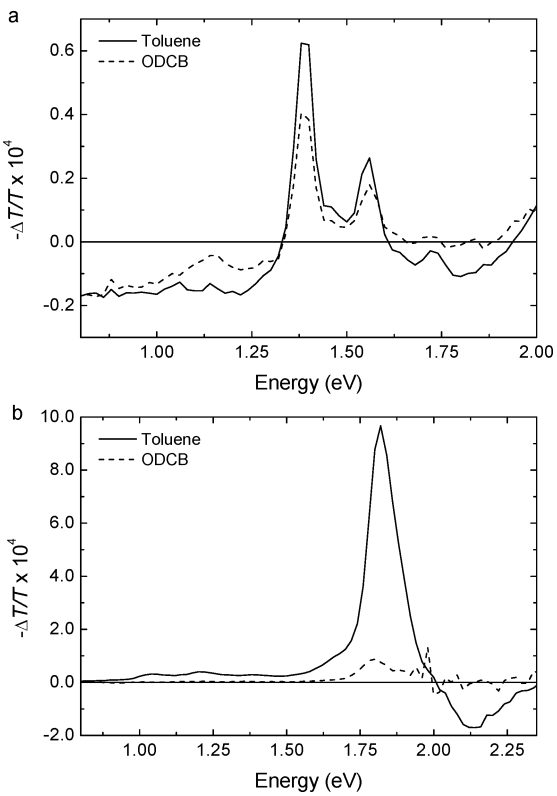

Fig. 5 Near steady-state PIA spectra of **DPP-T1-C_{60}** (a) and **DPP-T2-C_{60}** (b) recorded in toluene and ODCB, at an excitation wavelength of 514 nm.

singlet excited state of the DPP-oligomer. This process can either be triplet sensitization by the MP-C_{60} part of the molecules, as shown previously for mixtures of the oligomers and MP-C_{60}, or recombination of the charge separated state into the triplet state of the oligomer. The latter is possible *via* intersystem crossing (ISC) in the charge separated state, provided that the lifetime of this state is long enough. The fact that triplet excited oligomers are still observed in ODCB, with full quenching of the MP-C_{60} fluorescence, is in correspondence with the latter explanation. The smaller amount of observed triplets, reflected in the weaker signal, could be explained by the shorter lifetime of the charge separated state that is expected in ODCB, compared to toluene. This is due to the previous observation that charge recombination in this kind of systems takes place in the Marcus-inverted regime, leading to a shorter lifetime for the thermodynamically more stable charge separated state in ODCB.[48]

To obtain more insight into the processes occurring after excitation of the triads, the compounds were investigated by femtosecond transient absorption spectroscopy (fs-TA). fs-TA spectra of the oligomers in ODCB are shown in Fig. 6. For both compounds, a negative band consisting of the ground state bleaching and stimulated emission (SE) peaks (visible as the low-energy shoulder), and positive bands at lower and higher energy were observed. The latter bands can be attributed to the $S_n \leftarrow S_1$ absorptions of the oligomers. In both cases, the bands show a monoexponential decay, with a time constant of 3–4 ns, close to the fluorescence lifetimes of the oligomers determined by time-correlated single photon counting (Table 1). Fig. 6a shows that

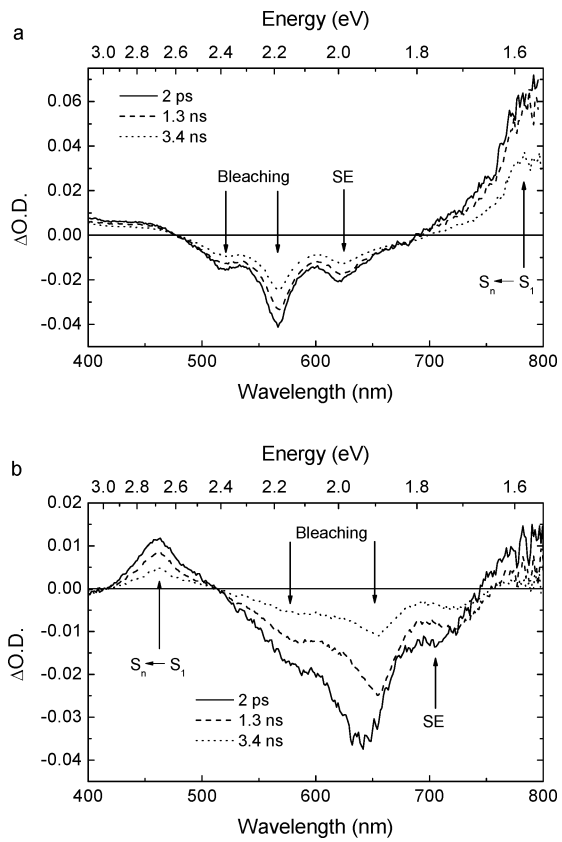

Fig. 6 fs-TA spectra of the oligomers **DPP-T1** (a) and **DPP-T2** (b) in ODCB.

for **DPP-T1** a low energy $S_n \leftarrow S_1$ transition is visible in the spectral window (400–800 nm). For **DPP-T2**, for which the normal absorption is at higher the wavelengths, the low energy $S_n \leftarrow S_1$ transition has shifted outside this region, while a high energy $S_n \leftarrow S_1$ transition appears in the spectral window. Based on the decay with time we attribute these bands to originate from the S_1 state of **DPP-T1** and **DPP-T2** respectively.

fs-TA data for the triads in toluene and ODCB are shown in Fig. 7. fs-TA spectra of **DPP-T1-C_{60}** in toluene could not be recorded, due to the very low solubility of the triad in that solvent. In all spectra shown in Fig. 7, the initially formed singlet excited state of the DPP-oligomer has decayed within 2 ps, as evidenced from the absence of the stimulated emission feature in the negative band. Therefore, the observed bleaching band is associated with the formation of the charge separated state (CSS), in which an electron has been transferred from the oligomer to the MP-C_{60} unit. In the next 20–140 ps, an increase of the bleaching band is observed, combined with a concomitant rise of absorptions in the regions where the cations of the oligomers absorb. This is due to charge separation from the singlet excited state of the MP-C_{60} unit, which has formed within the first ~0.5 picoseconds. The formed charged separated state then recombines partially to the ground state, and partially to the triplet excited state of the DPP oligomer. This is evidenced by the clear signal observed after a few ns at 690 nm (1.8 eV) for **DPP-T2-C_{60}** (most clearly visible in toluene), which is at the same position as the triplet absorption of the bare oligomer. For **DPP-T1-C_{60}**, the triplet absorption itself is not observed, as it is probably too weak, but the bleaching band of the oligomer does not completely vanish, indicating the presence of a long-lived excited state.

A schematic depiction of the charge separation and recombination process, following from the discussion above, is depicted in Fig. 8. In summary, excitation of the DPP-oligomer leads to partial charge transfer and partial energy transfer to the fullerene. The excited C_{60} moiety then leads to electron transfer from the DPP-oligomer to the fullerene, yielding the (singlet) charge separated state (^{1}CSS). This charge separated state then recombines to the ground state, or intersystem crossing to the lower energy triplet charge separated state (^{3}CSS) occurs, which recombines into the triplet excited state of the DPP oligomer. It has to be noted that the ^{3}CSS is not detected as a separate species because its formation (from ^{1}CSS) is much slower than its decay (to the triplet state localized on the DPP oligomer). Its intermediacy is assumed.

To access the rates for the different charge separation and recombination processes, global analysis of the data using the Glotaran[55] software has been performed. In this procedure, the time traces at all wavelengths are simultaneously fitted to a triexponential model. In case of **DPP-T2-C_{60}** in toluene, only 3 time traces (shown in Fig. 7f), characteristic for the different excited states, were fitted, because the global analysis did not converge. This procedure yielded time constants for charge separation (τ_{CS}^{C60}), charge recombination (τ_{CR}) and a very long component for the decay of the long-living triplet state of the oligomer. The time constants for charge separation and recombination are summarized in Table 3. Time constants for energy transfer from the initially formed singlet excited DPP unit to C_{60} (τ_{ET}) and for charge transfer from the same state (τ_{CS}^{DPP}) fall within the time resolution of the fs-TA setup (0.2 ps), but their spectral characteristics were obscured by the coherent artifact (pulse related phenomena).

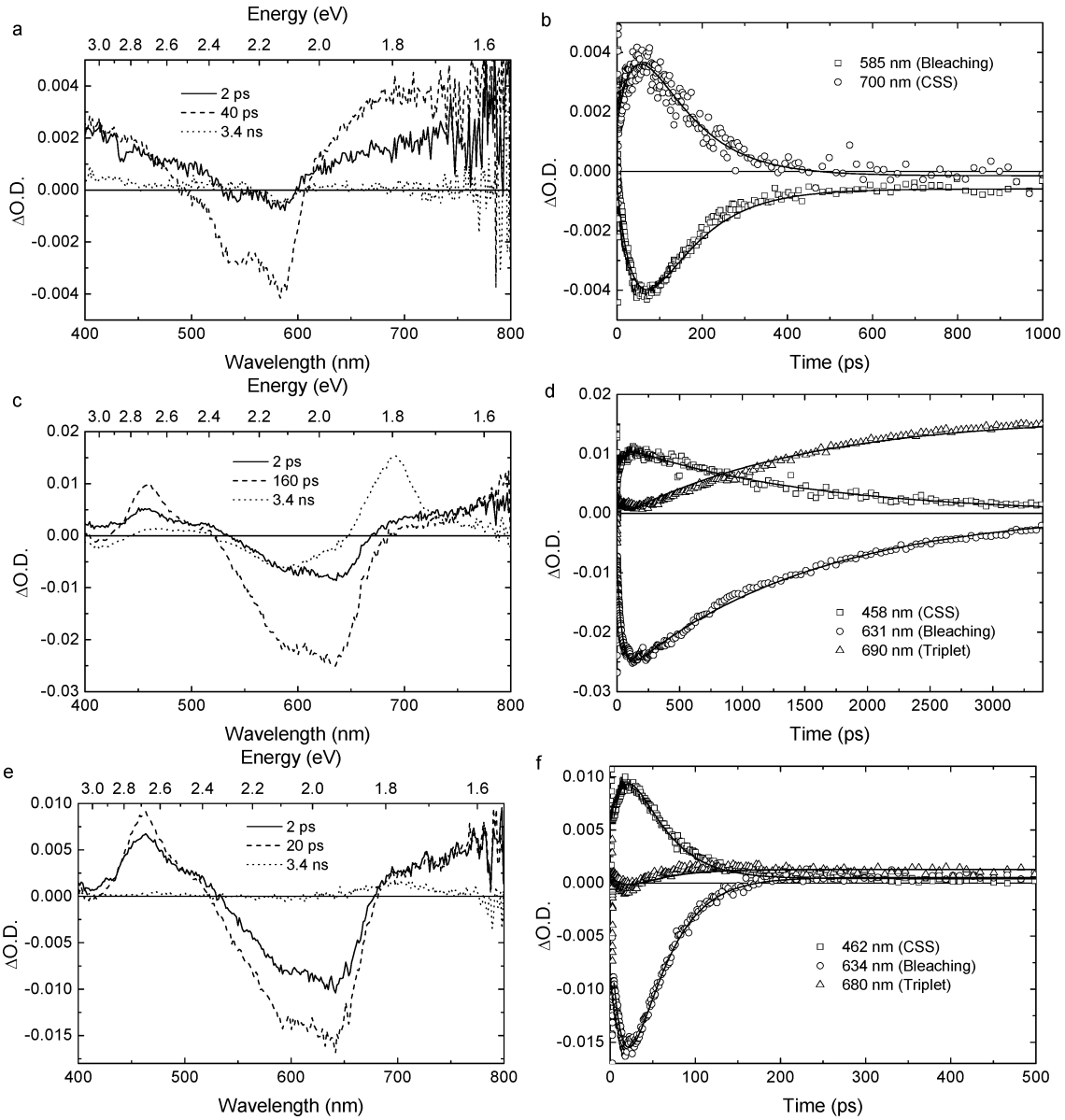

Fig. 7 fs-TA data for **DPP-T1-C_{60}** in ODCB (a, b) and **DPP-T2-C_{60}** in toluene (c, d) and ODCB (e, f). Graphs a, c, e show the evolution of the spectra with time, graphs b, d, f show time traces at selected wavelengths. The solid lines in the latter graphs are triexponential fits of the data, obtained by a global analysis procedure.

Table 3 Time constants for charge separation in the triad from the excited C_{60} unit ($\tau_{CS}{}^{C60}$), and recombination of the charges to either the ground state or the triplet excited state (τ_{CR})

	$\tau_{CS}{}^{C60}$/ps		τ_{CR}/ps	
	toluene	ODCB	toluene	ODCB
DPP-T1-C_{60}		47		110
DPP-T2-C_{60}	41	18	1500	37

Fitting the time traces results in only one, overall time constant (τ_{CR}) for charge recombination. From the scheme in Fig. 8 however, it is clear that this time constant is composed of the time constants for two different processes: recombination into the ground state (with $\tau_{CR}{}^{S}$) and recombination into a triplet state (with τ_{ISC}, provided that ISC is the rate limiting step for charge recombination into the triplet). A rough estimate of the quantum yield for charge recombination into the triplet state from the charge separated state can be made, by looking at the residual bleaching of the oligomer at long times. This bleaching, divided by the maximum bleaching obtained, is approximately equal to the fraction of the charge separated molecules that recombines into the triplet state. For **DPP-T1-C_{60}** in ODCB, approximately 14% of the formed charge separated states recombines into the triplet, meaning that $\tau_{CR}{}^{S}$ is about 6 times smaller than τ_{ISC} (*i.e.* recombination into the ground state is 6 times faster than ISC), resulting in τ_{ISC} of about 0.8 ns, using the relation:

$$\frac{1}{\tau_{CR}} = \frac{1}{\tau_{CR}^{S}} + \frac{1}{\tau_{ISC}} \quad (1)$$

Table 4 Singlet (E_{S1}) and triplet (E_{T1}) energy levels, half-wave oxidation potentials (E_{ox}, *vs.* Fc/Fc^+ in ODCB), cation radius (r^+), distance between positive and negative charges (R_{cc}), energy of the charge separated state (E_{CSS}) and free energies (ΔG) for the different charge separation and recombination processes (using the same sub- and superscripts as in Fig. 8). Energies are calculated for toluene and ODCB when the center of the positive charge is located on the center of the oligomer ("DPP") or on the thiophene/bithiophene unit next to the fullerene ("T")

	E_{S1}/eV	E_{T1}/eV	E_{ox}/V	r^+/Å	Location charge	R_{cc}/Å	Solvent	E_{CSS}/eV	ΔG_{CS}^{DPP}/eV	ΔG_{CS}^{C60}/eV	ΔG_{CR}^{S}/eV	ΔG_{CS}^{T}/eV
DPP-T1-C_{60}	2.15	1.1	0.46	4.3	DPP	9.7	toluene	1.79	–0.36	0.09	–1.79	–0.69
							ODCB	1.51	–0.64	–0.19	–1.51	–0.41
					T	6.9	toluene	1.62	–0.53	–0.08	–1.62	–0.52
							ODCB	1.45	–0.70	–0.25	–1.45	–0.35
DPP-T2-C_{60}	1.88	0.9	0.29	5.0	DPP	13.1	toluene	1.69	–0.19	–0.01	–1.69	–0.79
							ODCB	1.38	–0.50	–0.32	–1.38	–0.48
					T	8.5	toluene	1.52	–0.36	–0.18	–1.52	–0.62
							ODCB	1.32	–0.56	–0.38	–1.32	–0.72

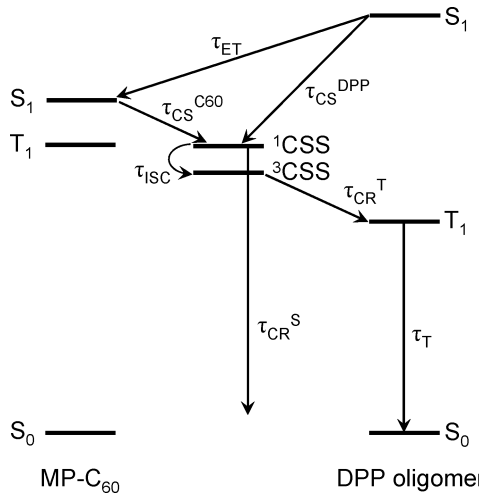

Fig. 8 Schematic depiction of the charge separation and recombination processes occurring after excitation of the triads. We note that the actual energy difference between ^{1}CSS and ^{3}CSS is not known and the difference shown in the graph is for clarity only.

For **DPP-T2-C_{60}** in toluene, the fraction of charge separated molecules that recombine into the triplet state is about 10%, meaning that τ_{CR}^{S} is about 9 times smaller than τ_{ISC}, resulting in τ_{ISC} of about 15 ns. For **DPP-T2-C_{60}** in ODCB, this analysis could not be performed, as the fraction recombination into triplet states is too small, due to the short lifetime of the charge separated state.

The energy of the charge separated state (E_{CSS}) in different solvents can be calculated with the following equation, based on a continuum model:[56]

$$E_{CSS} = e\left(E_{ox}(D) - E_{red}(A)\right) - \frac{e^2}{4\pi\varepsilon_0\varepsilon_s R_{cc}} - \frac{e^2}{8\pi\varepsilon_0}\left(\frac{1}{r^+}+\frac{1}{r^-}\right)\left(\frac{1}{\varepsilon_{ref}}-\frac{1}{\varepsilon_s}\right) \quad (2)$$

In this equation, $E_{ox}(D)$ is the oxidation potential of the oligomer and $E_{red}(A)$ is the reduction potential of MP-C_{60} (–1.2 V *vs.* Fc/Fc^+ in ODCB). R_{cc} is the center-to-center distance of the positive and negative charges, which was determined for the triads using molecular modeling, assuming the positive charge to be located either on the center of the oligomer (the DPP-unit) or asymmetrically on the center of the thiopene/bithiophene unit next to the fullerene, and the negative charge at the center of the fullerene moiety. r^+ and r^- are the radii of the positive and negative ions formed. r^- is calculated in literature to be 5.6 Å for C_{60}, based on the density of C_{60}.[15] r^+ can be estimated using a similar approach, using a density of 1.5, the value for unsubstituted terthiophene.[57] ε_{ref} and ε_s are the permittivities of the reference solvent (used to measure oxidation and reduction potentials) and the solvent in which electron transfer is studied. It is well known that solvents like toluene, with a low dipole moment and a high quadrupole moment, often show larger stabilization energies of charge separated states than predicted from their "bulk" relative permittivity. Because the relative permittivity does not describe the solvent-molecule interactions in these solvents well, an *apparent* permittivity can be used, such that the solvent behaves as a hypothetical solvent of polarity ε_{app}. For toluene, an apparent permittivity of 3.5 was used.[58,59] Values calculated for r^+, R_{cc}, E_{CSS}, and ΔG for the different charge transfer processes are summarized in Table 4.

Marcus theory estimates the activation barrier for photoinduced charge separation based on the free energy for charge separation, ΔG_{CS}, and the reorganization energy, *i.e.* the energy needed to deform the excited donor–acceptor system to the geometry of the charge separated state. Assuming the same parabolic energy curves for both the initial excited state and the charge separated state, this leads to:[60,61]

$$\Delta G_{CS}^{\ddagger} = \frac{\left(\Delta G_{CS} + \lambda\right)^2}{4\lambda} \quad (3)$$

where λ is the sum of internal (λ_i) and solvent (λ_s) contributions. The internal reorganization energy is set to 0.3 eV in this case, based on the reported value for the C_{60}/diethylaniline couple.[15] The solvent contribution can be calculated using the Born-Hush approach:[62]

$$\lambda_s = \frac{e^2}{4\pi\varepsilon_0}\left[\frac{1}{2}\left(\frac{1}{r^+}+\frac{1}{r^-}\right)-\frac{1}{R_{cc}}\right]\left(\frac{1}{n^2}-\frac{1}{\varepsilon_s}\right) \quad (4)$$

In this formula, n is the refractive index of the solvent, and the other parameters are the same as defined before. Reaction rates can be calculated using the non-adiabatic electron transfer theory by Jortner *et al.*:[63,64]

$$k_0 = \sqrt{\frac{\pi}{\hbar^2\lambda_s k_B T}}V^2\sum_{n=0}^{\infty}e^{-S}\frac{S^n}{n!}\exp\left(-\frac{\left(\Delta G_0+\lambda_s+n\hbar\omega\right)^2}{4\lambda_s k_B T}\right) \quad (5)$$

Table 5 Reorganization energy (λ), activation barriers ($\Delta G^{\ddagger}$) and calculated rate constants (k/V^2) for the different charge transfer processes (using the same sub- and superscripts as in Fig. 8), in toluene and ODCB when the center of the positive charge is located on the center of the oligomer ("DPP") or on the thiophene/bithiophene unit next to the fullerene ("T")

	Location charge	Solvent	λ/eV	$\Delta G^{\ddagger}_{CS}{}^{DPP}$/eV	$\Delta G^{\ddagger}_{CS}{}^{C60}$/eV	$\Delta G^{\ddagger}_{CR}{}^{S}$/eV	$\Delta G^{\ddagger}_{CR}{}^{T}$/eV	$k_{CS}{}^{DPP}/V^2$/ s^{-1} eV^2	$k_{CS}{}^{C60}/V^2$/ s^{-1} eV^2	$k_{CR}{}^{S}/V^2$/ s^{-1} eV^2	$k_{CR}{}^{T}/V^2$/ s^{-1} eV^2
DPP-T1-C_{60}	DPP	toluene	0.54	0.015	0.18	0.73	0.011	1.0×10^{16}	2.0×10^{11}	1.0×10^{13}	1.1×10^{16}
		ODCB	0.77	0.006	0.11	0.18	0.041	1.1×10^{16}	8.0×10^{13}	6.8×10^{14}	2.5×10^{15}
	T	toluene	0.44	0.005	0.073	0.79	0.003	1.3×10^{16}	2.3×10^{14}	1.6×10^{13}	1.3×10^{16}
		ODCB	0.58	0.006	0.047	0.33	0.021	1.2×10^{16}	2.0×10^{15}	2.3×10^{14}	7.2×10^{15}
DPP-T2-C_{60}	DPP	toluene	0.56	0.060	0.13	0.56	0.022	9.5×10^{14}	8.9×10^{12}	3.2×10^{13}	8.5×10^{15}
		ODCB	0.81	0.031	0.076	0.099	0.034	3.8×10^{15}	4.7×10^{14}	2.0×10^{15}	3.3×10^{15}
	T	toluene	0.47	0.006	0.043	0.59	0.012	1.5×10^{16}	2.5×10^{15}	5.2×10^{13}	1.1×10^{16}
		ODCB	0.63	0.002	0.025	0.19	0.017	1.3×10^{16}	5.8×10^{15}	8.2×10^{14}	8.3×10^{15}

In this equation, V describes the electronic coupling between donor and acceptor and $S = \lambda_i/\hbar\omega$, the effective mode vibrational energy. $\hbar\omega$ was set to 0.186 eV (1500 cm^{-1}), a value characteristic for the carbon-carbon double bond stretching frequency. Because the value of V is not known in our case, rates are calculated as k/V^2. Values calculated for λ, $\Delta G^{\ddagger}$, and k/V^2 for the different charge transfer processes are summarized in Table 5.

From the values in Table 4 and Table 5, it is clear that for charge separation from the initial excited state on the oligomer, λ is close to $\Delta G_{CS}{}^{DPP}$. This means that this charge separation takes place close to the Marcus optimal region, leading to low activation barriers and very fast charge separation, in line with experimental observations. Charge separation when the excited state is located on the fullerene unit, is clearly located in the Marcus normal region ($-\Delta G_{CS}{}^{DPP} < \lambda$), reflected in higher activation barriers and lower charge transfer rates. The fact that this charge separation process takes place in the Marcus normal region also explains the experimental observation that this process is faster in ODCB (where the charge separated state is stabilized) than in toluene. Charge recombination to the ground state clearly takes place in the Marcus inverted region ($-\Delta G_{CR}{}^{S} > \lambda$) in agreement with previous observations.[15–43] Because this charge recombination is located in the inverted region, charge recombination is faster in ODCB than in toluene. In all cases the calculated $\Delta G^{\ddagger}_{CR}{}^{S}$ is larger than $\Delta G^{\ddagger}_{CS}{}^{C60}$, in line with experimental observations. Energetically, charge recombination to the triplet state again takes place close to the Marcus normal region, which would lead to very high reaction rates. The experimental observation of slow triplet recombination can however be explained by a rate-limiting ISC process, instead of a rate-limiting charge transfer process.

For the general trends discussed above, the location of the positive charge is not of great importance. When calculating rate constants, however, using eqn (5), it does matter if the charge is located on the center of the DPP-oligomer, or more asymmetrically on the center of the thiophene/bithiophene unit next to the fullerene. If rate constants are estimated using the value of R_{cc} calculated for the positive charge being located on the oligomer center, the general trends are not reproduced. Here, the calculated values for $k_{CR}{}^{S}/V^2$ are larger than $k_{CS}{}^{C60}/V^2$, in contrast to the experimental observation that charge recombination is slower than charge separation. Furthermore, when calculating V, by comparing the observed $1/\tau_{CS}{}^{C60}$ and the calculated $k_{CS}{}^{C60}/V^2$, values for V of 11 to 52 meV are obtained. These are unrealistically large, as values of a few meV are generally obtained for donor–acceptor dyads and triads.[16,59,65] Recalculating the values with a smaller R_{cc}, obtained by placing the positive charge on the center of the thiophene/bithiophene unit next to the fullerene, accurately reproduces the experimental trends. The calculation results in very fast initial charge separation from the excited oligomer, somewhat slower recombination from the excited fullerene, and even slower charge recombination to the ground state. Moreover, the obtained value for V is 3.2 ± 0.1 meV, which is completely in line with commonly observed values.[16,59,65] Therefore, we can conclude that the positive charge is most probably located on the thiophene/bithiophene unit next to the fullerene. This conclusion is consistent with the idea that the DPP units are electron deficient compared to the electron rich thiophene/bithiophenes and that radical cations are preferentially formed on the latter units. Furthermore, similar cationic charge localization on an oligomeric unit (influencing the center to center distance) has been suggested before to occur in perylene-monoimide/oligothiophene electron donor–acceptor systems.[66]

Conclusions

Triads consisting of DPP-containing oligomers, end capped with fullerenes were prepared and photoinduced energy and electron transfer reactions were investigated by photoluminescence, near steady-state PIA and fs-TA techniques. After excitation of the DPP oligomer, charge transfer takes place *via* two simultaneously occurring routes. The first route is direct electron transfer, in the Marcus optimal regime, from the excited DPP oligomer to the fullerene. The second route is a two-step process consisting of ultrafast energy transfer from the DPP-oligomer to the fullerene, followed by charge separation from the formed excited state. In the latter case, the charge transfer process occurs in the Marcus normal regime, with time constants in the range of 18–47 ps. The formed charge separated state subsequently recombines *via* two distinct pathways. The first pathway is direct recombination to the ground state, which occurs in the Marcus inverted region, with time constants in the range of 37 ps to 1.5 ns. Because the charge separated state has a lower energy in the more polar ODCB, this process is much faster in ODCB than in toluene. The other pathway consists of intersystem crossing in the charge separated state, with time constants of 0.8 to 15 ns, and subsequent recombination into the triplet excited state of the DPP oligomer. ISC in the charge separated state is the rate-limiting step in this process. Clear signals for the triplet absorption of the oligomer

could be observed by near steady-state PIA and fs-TA. As the ISC process is slow compared to direct recombination to the ground state, triplet recombination was found to be of more importance in toluene than in ODCB, because of the slower direct recombination process in toluene. Analysis of the observed rates by Marcus-Jortner theory leads to the conclusion that the positive charge in the charge separated state is most likely not located on the center of the DPP oligomer, but rather asymmetrically on the thiophene/bithiophene unit next to the fullerene.

Experimental

General methods

^{1}H-NMR and ^{13}C-NMR spectra were recorded on a 500 MHz NMR (Varian Unity Plus, 500 MHz for ^{1}H-NMR and 125 MHz for ^{13}C-NMR) in CS_2, using a D_2O insert for locking and shimming. Chemical shifts are reported in ppm downfield from tetramethylsilane (TMS). IR spectra were recorded on a Perkin Elmer 1600 FT-IR. Matrix-assisted laser desorption ionization time-of-flight (MALDI-TOF) mass spectrometry has been performed on a PerSeptive Biosystems Voyager-DE PRO spectrometer. Preparative HPLC was performed using a Cosmosil Buckyprep Waters packed column (10 × 250 mm), using toluene as the eluent at a flow rate of 5 mL min^{-1}. Analytical HPLC analysis was performed on a Hewlett Packard HP LC-Chemstation 3D (Agilent/HP1100 Series) using an analytical Cosmosil Buckyprep column (4.6 × 250 mm).

Cyclic voltammograms were recorded in an inert atmosphere with 0.1 M tetrabutyl ammonium hexafluorophosphate ($TBAPF_6$) in ODCB as supporting electrolyte. The working electrode was a platinum disc (0.2 cm^2) and the counter electrode was a silver electrode. The samples were measured using an Ag/AgCl reference electrode with Fc/Fc^+ as an internal standard using a μAutolab II with a PGSTAT30 potentiostat.

UV/vis/nearIR absorption spectra were recorded using a PerkinElmer Lambda 900 spectrophotometer. Fluorescence spectra were recorded on an Edinburgh Instruments FS920 double-monochromator spectrophotometer with a Peltier-cooled red-sensitive photomultiplier. The emission spectra were corrected for the wavelength dependence of the sensitivity of the detection system. Time-correlated single photon counting fluorescence studies were performed on an Edinburgh Instruments LifeSpec-PS spectrometer by photoexcitation with a 400 nm picosecond laser (PicoQuant PDL 800B) operated at 2.5 MHz and by detection with a Peltier-cooled Hamamatsu microchannel plate photomultiplier (R3809U-50). The data were deconvoluted with the instrument response function of the instrument, recorded using dispersed light, and fitted to a monoexponential function using the Fluofit package (PicoQuant, Berlin).

Near-steady state PIA spectra were recorded by exciting with a mechanically modulated cw Ar-ion laser ($\lambda = 351$ and 364 nm or 514 nm, 275 Hz) pump beam and monitoring the resulting change in transmission of a tungsten-halogen probe light through the sample (ΔT) with a phase-sensitive lock-in amplifier after dispersion by a grating monochromator and detection, using Si, InGaAs, and cooled InSb detectors. The pump power incident on the sample was typically 25 mW with a beam diameter of 2 mm. The PIA ($\Delta T/T$) was corrected for the photoluminescence, which was recorded in a separate experiment. Photoinduced absorption spectra and photoluminescence spectra were recorded with the pump beam in a direction almost parallel to the direction of the probe beam. The solutions were studied in a 1 mm near-IR grade quartz cell at room temperature.

Femtosecond transient absorption experiments were performed with a Spectra-Physics Hurricane Titanium:Sapphire regenerative amplifier system. The full spectrum setup was based on an optical parametric amplifier (Spectra-Physics OPA 800C) as the pump. The residual fundamental light, from the pump OPA, was used for white/probe light generation, which was detected with a CCD spectrograph (Ocean Optics) for Vis detection. The polarization of the pump light was controlled by a Berek Polarization Compensator (New Focus). The Berek-Polarizer was always included in the setup to provide the Magic-Angle conditions. The probe light was double-passed over a delay line (Physik Instrumente, M-531DD) that provides an experimental time window of 3.6 ns with a maximal resolution of 0.6 fs per step. The OPA was used to generate excitation pulses at 530 nm. The laser output was typically 3.5–5 μJ pulse^{-1} (130 fs FWHM) with a repetition rate of 1 kHz. The samples were placed into cells of 2 mm path length (Hellma) and were stirred with a downward projected PTFE shaft, using a direct drive spectro-stir (SPECTRO-CELL). This stir system was also used for the white light generation in a 2 mm water cell. For the optical layout see supporting information of reference 67. All photophysical data reported here have a 5 to 10% error limit. All experiments were performed at room temperature.

Materials

C_{60} and MP-C_{60} were obtained from Solenne, other chemicals were purchased from Acros or Aldrich and used without purification. Synthesis of compounds **DPP-TA1** and **DPP-TA2** has been reported previously.[68] Reactions were performed under a nitrogen atmosphere.

2′,2‴-[[2,5-Bis(2-ethylhexyl)pyrrolo[3,4-*c*]pyrrole-1,4(2*H*,5*H*)-dione-3,6-diyl]bis(4-octyl-5,2-thiophenediyl)]bis[1′,5′-dihydro-1′-methyl-2′*H*-[5,6]fullereno-C_{60}-I_h-[1,9-*c*]pyrrole] (DPP-T1-C_{60}). Compound **DPP-TA1** (50 mg, 0.086 mmol), C_{60} (0.63 g, 0.87 mmol) and *N*-methylglycine (77 mg, 0.87 mmol) were dissolved in ODCB (125 mL). The mixture was stirred at 120 °C for 5 h. The reaction mixture was concentrated *in vacuo* and purified by column chromatography on silica, using CS_2 as the eluent to remove unreacted C_{60}, the product was subsequently eluted with toluene. Yield: 42 mg (40%). 14 mg of the product was further purified by preparative HPLC. ^{1}H-NMR (500 MHz, CS_2) δ (ppm): 8.92 (s, 2H, Ar-*H*), 5.32 (s, 2H, MP-*H*), 4.97 (d, $J = 9.0$ Hz, 2H, MP-*H*), 4.28 (d, $J = 10.0$ Hz, 2H, MP-*H*), 3.92 (m, 4H, -CH_2CH(C_4H_9)(C_2H_5)), 2.95 (s, 6H, N–CH_3). IR (cm^{-1}): 2948, 2923, 2856, 2782, 1668, 1574, 1456, 1091, 746, 736, 706. MALDI-TOF-MS *m/z* : 2074.39 (50%), 2075.36 (100), 2076.40 (90), 2077.37 (70), 2078.4 (40), 2079.38 (25). HPLC: 1 peak at 13.7 min.

2′,2‴-[[2,5-Bis(2-ethylhexyl)pyrrolo[3,4-*c*]pyrrole-1,4(2*H*,5*H*)-dione-3,6-diyl]bis(3′-octyl-5,5′-[2,2′-bithiophene]diyl)]bis[1′,5′-dihydro-1′-methyl-2′*H*-[5,6]fullereno-C_{60}-I_h-[1,9-*c*]pyrrole] (DPP-T2-C_{60}). Compound **DPP-TA2** (59 mg, 0.05 mmol), C_{60} (0.45 g, 0.62 mmol) and *N*-methylglycine (58 mg, 0.65 mmol) were

dissolved in ODCB (125 mL). The mixture was stirred at 120 °C for 5 h. The reaction mixture was concentrated *in vacuo* and purified by column chromatography on silica, using CS_2 as the eluent to remove unreacted C_{60}, the product was subsequently eluted with toluene–ethyl acetate. Yield: 95 mg (77%). 20 mg of the product was further purified by preparative HPLC. ^{1}H-NMR (500 MHz, CS_2) δ (ppm): 8.98 (d, $J = 4.1$ Hz, 2H, Ar-*H*), 7.20 (s, 2H, Ar-*H*), 7.18 (d, $J = 4.1$ Hz, 2H, Ar-*H*), 5.14 (s, 2H, MP-*H*), 4.93 (d, $J = 9.5$ Hz, 2H, MP-*H*), 4.23 (d, $J = 9.5$ Hz, 2H, MP-*H*), 3.92 (d, $J = 7.5$ Hz, 4H, –CH_2CH(C_4H_9)(C_2H_5)), 2.93 (s, 6H, N–CH_3), 2.80 (t, $J = 7.3$ Hz, 4H, –C$H_2C_7H_{15}$), 1.84 (m, 2H, –CH$_2$CH(C_4H_9)(C_2H_5)), 1.63 (m, 4H, –CH$_2$C$H_2C_6H_{13}$), 1.40–1.16 (m, 36H, –CH_2–), 0.92–0.82 (m, 18H, –CH_3). ^{13}C-NMR (125 MHz, CS_2) δ (ppm): 160.61, 155.82, 153.76, 153.01, 152.83, 147.49, 146.85, 146.55, 146.51, 146.41, 146.39, 146.34, 146.29, 146.15, 145.92, 145.88, 145.83, 145.62, 145.57, 145.47, 145.44, 145.38, 144.92, 144.85, 144.57, 144.54, 143.38, 143.24, 142.94, 142.84, 142.47, 142.38, 142.30, 142.28, 142.24, 142.16, 142.14, 142.07, 141.88, 141.82, 141.45, 141.44, 140.47, 140.45, 140.22, 140.20, 139.96, 138.87, 137.31, 136.88, 136.86, 136.11, 135.78, 131.45, 130.74, 129.55, 129.54, 127.76, 126.87, 126.85, 108.73, 104.99, 79.30, 77.17, 70.27, 68.80, 45.83, 40.69, 39.76, 32.62, 30.85, 30.63, 30.38, 30.29, 30.25, 30.07, 28.96, 24.14, 24.11, 23.65, 14.96, 11.10. IR (cm^{-1}): 2951, 2922, 2851, 2781, 1663, 1543, 1456, 1429, 733. MALDI-TOF-MS *m*/*z*: 2462.50 (40%), 2463.50(80), 2464.49 (100), 2465.47 (80), 2466.46 (55), 2467.44 (30), 2468.43 (10). HPLC: 1 peak at 9.0 min.

Acknowledgements

The research was supported by a TOP grant of the Chemical Sciences (CW) division of the Netherlands Organization for Scientific Research (NWO) and is part of the Joint Solar Programme (JSP). The JSP is co-financed by the Foundation for Fundamental Research on Matter (FOM), Chemical Sciences of NWO, and the Foundation Shell Research. The work forms part of the research programme of the Dutch Polymer Institute (DPI, projects 524 and 631).

References

1 S. H. Park, A. Roy, S. Beaupré, S. Cho, N. Coates, J. S. Moon, D. Moses, M. Leclerc, K. Lee and A. J. Heeger, Bulk heterojunction solar cells with internal quantum efficiency approaching 100%, *Nat. Photonics*, 2009, **3**, 297–303.
2 Y. Liang, D. Feng, Y. Wu, S. T. Tsai, G. Li, C. Ray and L. Yu, Highly efficient solar cell polymers developed *via* fine-tuning of structural and electronic properties, *J. Am. Chem. Soc.*, 2009, **131**, 7792–7799.
3 J. Hou, H. Y. Chen, S. Zhang, R. I. Chen, Y. Yang, Y. Wu and G. Li, Synthesis of a low band gap polymer and its application in highly efficient polymer solar cells, *J. Am. Chem. Soc.*, 2009, **131**, 15586–15587.
4 Y. Liang, Z. Xu, J. Xia, S. T. Tsai, Y. Wu, G. Li, C. Ray and L. Yu, For the bright future - bulk heterojunction polymer solar cells with power conversion efficiency of 7.4%, *Adv. Mater.*, 2010, **22**, E135–E138.
5 M. M. Wienk, M. Turbiez, J. Gilot and R. A. J. Janssen, Narrow-bandgap diketo-pyrrolo-pyrrole polymer solar cells: The effect of processing on the performance, *Adv. Mater.*, 2008, **20**, 2556–2560.
6 J. C. Bijleveld, A. P. Zoombelt, S. G. J. Mathijssen, M. M. Wienk, M. Turbiez, D. M. de Leeuw and R. A. J. Janssen, Poly(diketopyrrolopyrrole–terthiophene) for ambipolar logic and photovoltaics, *J. Am. Chem. Soc.*, 2009, **131**, 16616–16617.
7 Y. Zou, D. Gendron, R. Neagu-Plesu and M. Leclerc, Synthesis and characterization of new low-bandgap diketopyrrolopyrrole-based copolymers, *Macromolecules*, 2009, **42**, 6361–6365.
8 E. Zhou, Q. Wei, S. Yamakawa, Y. Zhang, K. Tajima, C. Yang and K. Hashimoto, Diketopyrrolopyrrole-based semiconducting polymer for photovoltaic device with photocurrent response wavelengths up to 1.1 μm, *Macromolecules*, 2010, **43**, 821–826.
9 A. B. Tamayo, B. Walker and T. Q. Nguyen, A low band gap, solution processable oligothiophene with a diketopyrrolopyrrole core for use in organic solar cells, *J. Phys. Chem. C*, 2008, **112**, 11545–11551.
10 A. B. Tamayo, X. D. Dang, B. Walker, J. Seo, T. Kent and T. Q. Nguyen, A low band gap, solution processable oligothiophene with a dialkylated diketopyrrolopyrrole chromophore for use in bulk heterojunction solar cells, *Appl. Phys. Lett.*, 2009, **94**, 103301.
11 B. Walker, A. B. Tamayo, X. D. Dang, P. Zalar, J. H. Seo, A. Garcia, M. Tantiwiwat and T. Q. Nguyen, Nanoscale phase separation and high photovoltaic efficiency in solution-processed, small-molecule bulk heterojunction solar cells, *Adv. Funct. Mater.*, 2009, **19**, 3063–3069.
12 T. A. Ford, I. Avilov, D. Beljonne and N. C. Greenham, Enhanced triplet exciton generation in polyfluorene blends, *Phys. Rev. B: Condens. Matter Mater. Phys.*, 2005, **71**, 125212.
13 T. Offermans, P. A. van Hal, S. C. J. Meskers, M. M. Koetse and R. A. J. Janssen, Exciplex dynamics in a blend of pi-conjugated polymers with electron donating and accepting properties: MDMO-PPV and PCNEPV, *Phys. Rev. B: Condens. Matter Mater. Phys.*, 2005, **72**, 045213.
14 T. A. Ford, H. Ohkita, S. Cook, J. R. Durrant and N. C. Greenham, Direct observation of intersystem crossing in charge-pair states in polyfluorene polymer blends, *Chem. Phys. Lett.*, 2008, **454**, 237–241.
15 R. M. Williams, J. M. Zwier and J. W. Verhoeven, Photoinduced intramolecular electron transfer in a bridged C60 (acceptor)-aniline (donor) system; Photophysical properties of the first "active" fullerene diad, *J. Am. Chem. Soc.*, 1995, **117**, 4093–4099.
16 H. Imahori, S. Cardoso, D. Tatman, S. Lin, L. Noss, G. R. Seely, L. Sereno, J. Chessa, de Silber, T. A. Moore, A. L. Moore and D. Gust, Photoinduced electron transfer in a carotenobuckministerfullerene dyad, *Photochem. Photobiol.*, 1995, **62**, 1009–1014.
17 R. M. Williams, M. Koeberg, J. M. Lawson, Y. Z. An, Y. Rubin, M. N. PaddonRow and J. W. Verhoeven, Photoinduced electron transfer to C-60 across extended 3- and 11-bond hydrocarbon bridges: Creation of a long-lived charge-separated state, *J. Org. Chem.*, 1996, **61**, 5055–5062.
18 P. A. Liddell, D. Kuciauskas, J. P. Sumida, B. Nash, D. Nguyen, A. L. Moore, T. A. Moore and D. Gust, Photoinduced charge separation and charge recombination to a triplet state in a carotene-porphyrin-fullerene triad,, *J. Am. Chem. Soc.*, 1997, **119**, 1400–1405.
19 H. Imahori, K. Yamada, M. Hasegawa, S. Taniguchi, T. Okada and Y. Sakata, A sequential photoinduced electron relay accelerated by fullerene in a porphyrin-pyromellitimide-C60 triad, *Angew. Chem., Int. Ed. Engl.*, 1997, **36**, 2626–2629.
20 H. Imahori and Y. Sakata, Donor-linked fullerenes. Photoinduced electron transfer and its potential application, *Adv. Mater.*, 1997, **9**, 537–547.
21 D. M. Guldi, M. Maggini, G. Scorrano and M. Prato, Intramolecular electron transfer in fullerene/ferrocene based donor–bridge–acceptor dyads, *J. Am. Chem. Soc.*, 1997, **119**, 974–980.
22 D. M. Guldi and K. D. Asmus, Photophysical properties of mono- and multiply-functionalized fullerene derivatives, *J. Phys. Chem. A*, 1997, **101**, 1472–1481.
23 N. Martín, L. Sánchez, B. Illescas and I. Pérez, C60-Based electroactive organofullerenes, *Chem. Rev.*, 1998, **98**, 2527–2547.
24 H. Imahori and Y. Sakata, Fullerenes as novel acceptors in photosynthetic electron transfer, *Eur. J. Org. Chem.*, 1999, 2445–2457.
25 N. V. Tkachenko, L. Rantala, A. Y. Tauber, J. Helaja, P. H. Hynninen and H. Lemmetyinen, Photoinduced electron transfer in phytochlorin-[60] fullerene dyads, *J. Am. Chem. Soc.*, 1999, **121**, 9378–9387.
26 D. I. Schuster, P. Cheng, S. R. Wilson, V. Prokhorenko, M. Katterle, A. R. Holzwarth, S. E. Braslavsky, G. Klihm, R. M. Williams and C. P. Luo, Photodynamics of a constrained parachute-shaped fullerene-porphyrin dyad, *J. Am. Chem. Soc.*, 1999, **121**, 11599–11600.
27 D. M. Guldi and M. Prato, Excited-state properties of C60 fullerene derivatives, *Acc. Chem. Res.*, 2000, **33**, 695–703.
28 J. F. Eckert, J. F. Nicoud, J. F. Nierengarten, S. G. Liu, L. Echegoyen, F. Barigelletti, N. Armaroli, L. Ouali, V. V. Krasnikov and G. Hadziioannnou, Fullerene-oligophenylenevinylene hybrids: synthesis, electronic properties, and incorporation in photovoltaic devices, *J. Am. Chem. Soc.*, 2000, **122**, 7467–7479.
29 E. Peeters, P. A. van Hal, J. Knol, C. J. Brabec, N. S. Sariciftci, J. C. Hummelen and R. A. J. Janssen, Synthesis, photophysical

properties, and photovoltaic devices of oligo(p-phenylene vinylene)-fullerene dyads, *J. Phys. Chem. B*, 2000, **104**, 10174–10190.
30 C. Luo, D. M. Guldi, H. Imahori, K. Tamaki and K. Sakata, Sequential energy and electron transfer in an artificial reaction center: Formation of a long-lived charge-separated state, *J. Am. Chem. Soc.*, 2000, **122**, 6535–6551.
31 J.L. Bahr, D. Kuciauskas, P. A. Liddell, A. L. Moore, T. A. Moore and D. Gust, Driving force and electronic coupling effects on photoinduced electron transfer in a fullerene-based molecular triad, *Photochem. Photobiol.*, 2000, **72**, 598–611.
32 H. Imahori, K. Tamaki, D. M. Guldi, C. P. Luo, M. Fujitsuka, O. Ito, Y. Sakata and S. Fukuzumi, Modulating charge separation and charge recombination dynamics in porphyrin fullerene linked dyads and triads: Marcus-normal *versus* inverted region, *J. Am. Chem. Soc.*, 2001, **123**, 2607–2617.
33 D. Gust, T. A. Moore and A. L. Moore, Mimicking photosynthetic solar energy transduction, *Acc. Chem. Res.*, 2001, **34**, 40–48.
34 S. Fukuzumi, K. Ohkubo, H. Imahori, J. G. Shao, Z. P. Ou, G. Zheng, Y. H. Chen, R. K. Pandey, M. Fujitsuka, O. Ito and K. M. Kadish, Photochemical and electrochemical properties of zinc chlorin-C60 dyad as compared to corresponding free-base chlorin-C60, free-base Porphyrin-C60, and zinc porphyrin-C60 dyads, *J. Am. Chem. Soc.*, 2001, **123**, 10676–10683.
35 D. M. Guldi, Fullerene-porphyrin architectures; photosynthetic antenna and reaction center models, *Chem. Soc. Rev.*, 2002, **31**, 22–36.
36 T. J. Kesti, N. V. Tkachenko, V. Vehmanen, H. Yamada, H. Imahori, S. Fukuzumi and H. Lemmetyinen, Exciplex intermediates in photoinduced electron transfer of porphyrin- fullerene dyads, *J. Am. Chem. Soc.*, 2002, **124**, 8067–8077.
37 P. A. Liddell, G. Kodis, A. L. Moore, T. A. Moore and D. Gust, Photonic switching of photoinduced electron transfer in a dithienylethene-porphyrin-fullerene triad molecule, *J. Am. Chem. Soc.*, 2002, **124**, 7668–7669.
38 D. I. Schuster, P. Cheng, P. D. Jarowski, D. M. Guldi, C. P. Luo, L. Echegoyen, S. Pyo, A. R. Holzwarth, S. E. Braslavsky, R. M. Williams and G. Klihm, Design, synthesis, and photophysical studies of a porphyrin-fullerene dyad with parachute topology; Charge recombination in the Marcus inverted region, *J. Am. Chem. Soc.*, 2004, **126**, 7257–7270.
39 J. L. Segura, N. Martín and D. M. Guldi, Materials for organic solar cells: the C60/π-conjugated oligomer approach, *Chem. Soc. Rev.*, 2005, **34**, 31–47.
40 D. M. Guldi, A. Rahman, V. Sgobba and C. Ehli, Multifunctional molecular carbon materials - from fullerenes to carbon nanotubes, *Chem. Soc. Rev.*, 2006, **35**, 471–487.
41 D. I. Schuster, K. Li, D. M. Guldi, A. Palkar, L. Echegoyen, C. Stanisky, R. J. Cross, M. Niemi, N. V. Tkachenko and H. Lemmetyinen, azobenzene-linked porphyrin- fullerene dyads, *J. Am. Chem. Soc.*, 2007, **129**, 15973–15982.
42 H. Imahori, Creation of fullerene-based artificial photosynthetic systems, *Bull. Chem. Soc. Jpn.*, 2007, **80**, 621–636.
43 D. M. Guldi, B. M. Illescas, C. M. Atienza, M. Wielopolskia and N. Martin, Fullerene for organic electronics, *Chem. Soc. Rev.*, 2009, **38**, 1587–1597.
44 J. W. Verhoeven, On the role of spin correlation in the formation, decay, and detection of long-lived, intramolecular charge-transfer states, *J. Photochem. Photobiol., C*, 2006, **7**, 40–60.
45 Z. E. X. Dance, Q. Mi, D. W. McCamant, M. J. Ahrens, M. A. Ratner and M. R. Wasielewski, Time-resolved EPR studies of photogenerated radical ion pairs separated by p-phenylene oligomers and of triplet states resulting from charge recombination, *J. Phys. Chem. B*, 2006, **110**, 25163–25173.
46 M. R. Wasielewski, D. G. Johnson, W. A. Svec, K. M. Kersey and D. W. Minsek, Achieving high quantum yield charge separation in porphyrin-containing donor–acceptor molecules at 10 K, *J. Am. Chem. Soc.*, 1988, **110**, 7219–7221.
47 G. P. Wiederrecht, W. A. Svec, M. R. Wasielewski, T. Galili and H. Levanon, Novel mechanism for triplet state formation in short distance covalently linked radical ion pairs, *J. Am. Chem. Soc.*, 2000, **122**, 9715–9722.
48 B. P. Karsten, R. K. M. Bouwer, J. C. Hummelen, R. M. Williams and R. A. J. Janssen, Charge separation and recombination in small band gap oligomer - fullerene triads, *J. Phys. Chem. B*, 2010, **114**, DOI: 10.1021/jp906973d.
49 A. B. Tamayo, M. Tantiwiwat, B. Walker and T. Q. Nguyen, Design, synthesis, and self-assembly of oligothiophene derivatives with a diketopyrrolopyrrole core, *J. Phys. Chem. C*, 2008, **112**, 15543–15552.
50 M. Maggini, G. Scorrano and M. Prato, Addition of azomethine ylides to C60: synthesis, characterization, and functionalization of fullerene pyrrolidines, *J. Am. Chem. Soc.*, 1993, **115**, 9798–9799.
51 P. A. van Hal, E. H. A. Beckers, E. Peeters, J. J. Apperloo and R. A. J. Janssen, Photoinduced intermolecular electron transferbetween oligo(p-phenylene vinylene)s and N-methylfulleropyrrolidine in a polar solvent, *Chem. Phys. Lett.*, 2000, **328**, 403–408.
52 W. G. Herkstroeter and P. B. Merkel, The triplet state energies of rubrene and diphenylisobenzofuran, *J. Photochem.*, 1981, **16**, 331–341.
53 P. A. Firey, W. E. Ford, J. R. Sounik, M. E. Kenney and M. A. J. Rodgers, Silicon naphthalocyanine triplet state and oxygen. A reversible energy-transfer reaction, *J. Am. Chem. Soc.*, 1988, **110**, 7626–7630.
54 H. J. Shine, B. J. Zhao, J. N. Marx, T. Ould-Ely and K. H. Whitmire, Decomposition of alkene adducts of thianthrene cation radical in nitrile solvents. formation of alkyl-2-oxazolines and a new class of four-component products: 5-[(1-Alkoxyalkylidene)ammonio]alkylthianthrenium diperchlorates, *J. Org. Chem.*, 2004, **69**, 9255–9261.
55 *Glotaran 0.2.1*, http://timpgui.org/, a graphical user interface for the R-package TIMP: K. M. Mullen and I. H. M. van Stokkum, TIMP: An R Package for Modeling Multi-way Spectroscopic Measurements, *J. Stat. Software*, 2007, **18**, 1–46.
56 A. Weller, Photoinduced electron-transfer in solution - exciplex and radical ion-pair formation free enthalpies and their solvent dependence, *Z. Phys. Chem. Neue Folge*, 1982, **133**, 93–98.
57 F. van Bolhuis, H. Wynberg, E. E. Havinga, E. W. Meijer and E. G. J. Staring, The X-ray structure and MNDO calculations of α-terthienyl: A model for polythiophenes, *Synth. Met.*, 1989, **30**, 381–389.
58 L. Reynolds, J. A. Gardecki, S. J. V. Frankland, M. L. Horng and M. Maroncelli, Dipole solvation in nondipolar solvents: experimental studies of reorganization energies and solvation dynamics, *J. Phys. Chem.*, 1996, **100**, 10337–10354.
59 D. Veldman, S. M. A. Chopin, S. C. J. Meskers and R. A. J. Janssen, Enhanced intersystem crossing *via* a high energy charge transfer state in a perylenediimide– perylenemonoimide dyad, *J. Phys. Chem. A*, 2008, **112**, 8617–8632.
60 R. A. Marcus, On theory of electron-transfer reactions. VI. Unified treatment for homogeneous and electrode reactions, *J. Chem. Phys.*, 1965, **43**, 679–701.
61 R. A. Marcus, Electron-transfer reactions in chemistry - theory and experiment (Nobel lecture), *Angew. Chem., Int. Ed. Engl.*, 1993, **32**, 1111–1121.
62 H. Oevering, M. N. Paddon-Row, M. Heppener, A. M. Oliver, E. Cotsaris, J. W. Verhoeven and N. S. Hush, Long-range photoinduced through-bond electron transfer and radiative recombination *via* rigid nonconjugated bridges: distance and solvent dependence, *J. Am. Chem. Soc.*, 1987, **109**, 3258–3269.
63 N. R. Kestner, J. Logan and J. Jortner, Thermal electron transfer reactions in polar solvents, *J. Phys. Chem.*, 1974, **78**, 2148–2166.
64 J. Ulstrup and J. Jortner, Effect of intramolecular quantum modes on free-energy relationshipsfor electron-transfer reactions, *J. Chem. Phys.*, 1975, **63**, 4358–4368.
65 E. H. A. Beckers, S. C. J. Meskers, A. P. H. J. Schenning, Z. J. Chen, F. Würthner and R. A. J. Janssen, Charge separation and recombination in photoexcited oligo(p-phenylene vinylene): Perylene bisimide arrays close to the marcus inverted region, *J. Phys. Chem. A*, 2004, **108**, 6933–6937.
66 A. Petrella, J. Cremer, L. de Cola, P. Bäuerle and R. M. Williams, Charge transfer processes in conjugated triarylamine-oligothiophene-perylenemonoimide dendrimers, *J. Phys. Chem. A*, 2005, **109**, 11687–11695.
67 J. Baffreau, S. Leroy-Lhez, N. Vân Anh, R. M. Williams and P. Hudhomme, Fullerene C-60-Perylene-3,4 : 9,10-bis(dicarboximide) light-harvesting dyads: Spacer-length and bay-substituent effects on intramolecular singlet and triplet energy transfer, *Chem.–Eur. J.*, 2008, **14**, 4974–4992.
68 B. P. Karsten, J. C. Bijleveld and R. A. J. Janssen, Diketopyrrolopyrroles as acceptor materials in organic photovoltaics, *Macromol. Rapid Comm.*, 2010, DOI: 10.1002/marc.201000133.